

CHEMOTROPISM INDICES FOR POLYMORPHONUCLEAR LEUKOCYTES

RALPH NOSSAL *and* SALLY H. ZIGMOND

From the Physical Sciences Laboratory, D.C.R.T., National Institutes of Health, Bethesda, Maryland 20014, and the Section of Cell Biology, Yale University Medical School, New Haven, Connecticut 06510. Dr. Zigmond's present address is Department of Biology, University of Pennsylvania, Philadelphia, Pennsylvania 19104.

ABSTRACT Trajectories of polymorphonuclear leukocytes which are responding to a chemical gradient are analyzed in order to deduce probability distributions of the angles between successive path segments. The turn-angle probability distributions thus obtained are seen to be strongly dependent on the direction of locomotion prior to a turn, in that cells usually turn to maintain alignment along an axis directed towards the chemoattractant source. A mathematical model based on these observations is developed in order to understand the relationship between net chemotactic response and parameters characterizing stochastic movements of individual cells. In particular, the manner in which the chemotropism index depends on details of the turn-angle distributions is examined. When bias in the direction of turn is induced by a chemotactic field, transition from random motion to directed response occurs most abruptly if the turn-angle distribution is narrow. "Accommodation," viz., a dependence of the mean angle of turn upon prior orientation, is found to have relatively little effect on the magnitude of the response.

INTRODUCTION

Polymorphonuclear (PMN) leukocytes have been shown to respond to a number of chemotactic stimuli. Examples include factors released by various bacteria (Ward et al., 1968), complement-derived peptides (Ward et al., 1966; Shin et al., 1968; Bokisch et al., 1969), factors released during blood coagulation (Stecher et al., 1971), "lymphokines" released by sensitized lymphocytes (Ward et al., 1969), substances produced by PMN cells, themselves, when they come into contact with certain particulate materials such as urate crystals or aggregated γ -globulin (Phelps, 1969; Zigmond and Hirsch, 1973), and certain synthetic peptides (Schiffmann et al., 1975). Although these responses have been investigated in vitro, motivation for such studies derives from observations of granulocyte migration into regions of tissue damage as an accompaniment of injury or infection (see, for example, Harris, 1960; Miller, 1973; Wilkinson, 1974).

The directed response of individual cells which are moving over a surface upon which a chemical field has been imposed is conveniently quantified by a "chemotropism index." The latter, as originally introduced by McCutcheon (1923), is defined

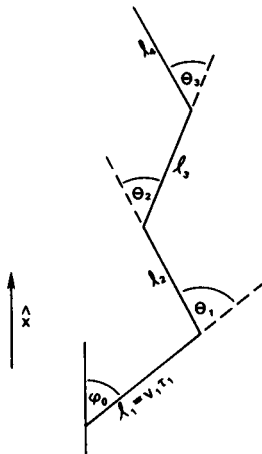


FIGURE 1 Schematic of cell locomotion. l_i is the length of the i th path segment and θ_i is the angle through which the cell turns before beginning the $(i + 1)$ st segment.

as the net path length traversed by a cell in the direction of the source divided by the total distance traveled. Thus, in terms of the scheme delineated in Fig. 1, the chemotropism index CI is given as

$$CI = \frac{\sum_{i=1}^N l_i \cos \varphi_i}{\sum_{i=1}^N l_i}, \quad (1)$$

where l_i is the length of the i^{th} path segment, and φ_i is the angle which that segment makes with the direction towards the source (here designated as the \hat{x} axis). The $\{\varphi_i\}$ can be expressed in terms of the angles between the $(i - 1)$ st and i th segments $\{\theta_i\}$ (see Fig. 1) according to

$$\varphi_i = \varphi_0 + \theta_1 + \dots + \theta_{i-1}, \quad (2)$$

where φ_0 is the angle pertaining to the initial movement of the cell.

One virtue of using the chemotropism index as an indicator of cell motion is the relative ease with which it is determined. Time-lapse cinemicrographs are projected sequentially, and the paths of individual cells traced. The index for each cell is calculated according to Eq. 1 and an averaged chemotropism index $\langle CI \rangle$ then is computed by summing the results for all cells and dividing by the total number. Note that the averaged chemotropism index will have the value $\langle CI \rangle = 1$ in the event that the cells are always moving towards the source; if, on the other hand, there is no preference for directional orientation, $\langle CI \rangle = 0$, due to the fact that on average there will be as many cells moving away from as there will be cells moving towards the source.

The chemotropism index $\langle CI \rangle$ is closely related to the directed (chemotactic) velocity v_d , the latter being given as (Nossal and Weiss, 1974a, b)

$$v_d = \lim_{t \rightarrow \infty} \left\{ t^{-1} \left\langle \sum_{i=1}^{N(t)} l_i \cos \varphi_i \right\rangle_t \right\}. \quad (3)$$

Suppose that the speed and duration of travel on the i th path segment are designated as v_i and τ_i , respectively; then, from Eq. 1 $\langle CI \rangle$ is given as

$$\langle CI \rangle \simeq t v_d / \left\langle \sum_{i=1}^N \tau_i v_i \right\rangle = v_d / \langle |v| \rangle \equiv a_0, \quad (4)$$

where the term in the denominator, $\langle |v| \rangle = t^{-1} \langle \sum_{i=1}^N \tau_i v_i \rangle$, is the speed of a typical cell averaged over its entire displacement. Implicit in the derivation of Eq. 4 is an assumption that the path segments are, individually, only weakly correlated with the total path length. (Intuitively, we expect this to be true when N becomes sufficiently large.)

The significance of Eq. 4 is that, when expressed in this manner, the chemotropism index may be computed from a theory which previously has been derived for relating macroscopic response to microscopic parameters pertaining to the stochastic motion of individual particles (Nossal, 1976; Nossal and Weiss, 1974b). Specifically, a_0 is given as the solution of the infinite set of equations

$$\frac{1}{2} [\beta_{m+1} + \beta_{m-1}] - a_0 \beta_m = \sum_{l=-\infty}^{\infty} b_l \{ \delta_{l,m}^{Kr} - p_{-l} I(m, 0, l) \}, \quad (5)$$

$$m = \dots -2, -1, 0, 1, 2 \dots$$

where the $\{b_l\}$ are subsidiary variables, and the coefficients $\{\beta_m\}$, $\{p_m\}$, and $I(m, 0, l)$ are derived from the probability distributions of the turn angles. A detailed discussion of Eq. 5 and its solution appears in the Calculations section below. There, we use an analytic representation for turning angle distributions which we deduce from previously published studies of granulocyte chemotaxis (Zigmond, 1974). In the Numerical Results section we examine different possibilities for chemotactic "triggering," and use numerical results to infer characteristics of turn-angle distributions which would optimize chemotactic responsiveness.

TURN-ANGLE PROBABILITIES

One of us (Zigmond, 1974) recently has used time-lapse cinemicrography to study the manner in which horse polymorphonuclear leukocytes sense chemical gradients. Cells were filmed as they moved in response to a chemotactic gradient generated by other leukocytes in contact with a streak of aggregated γ -globulin (Zigmond and Hirsch, 1973.) 30 cells were selected at random and their trajectories analyzed in detail from measurements of turn angles and path lengths (distances between turns).

Although the probability distribution for run-lengths $\{\tau_i\}$ in general might be a function of a cell's orientation when moving in the field (see, for example, Berg and Brown's [1972] studies of chemotactic bacteria), such did not seem to be the case for leukocyte chemotaxis. However, a strong correlation existed between the direction of a turn and a cell's prior orientation, so that the cells tended on the average to align themselves along the axis directed towards the source. In addition, a weak correlation was found between the magnitude of the turns and the cell orientations.

Here, we present the results of some further analysis of the trajectories of those cells upon which the above conclusions were based. We now are particularly interested in determining $p(\theta | \varphi)$, which is the probability that a cell will turn through an angle θ , given that it was moving at an angle φ with respect to the source axis before the turn.

Histograms of the tracking data were made by dividing the continuous domain of angles into a discrete mesh of 15° segments. Results are shown in Figs. 2a and b.¹ In Fig. 2a we plot, for illustration, the histogram of turn angles when cells were moving at an angle lying between 0° and 15° "off-axis." Note that when the prior movement of the cells was in a "positive" direction, they tended to turn through a negative angle, whereas if moving in a "negative" direction they tended to turn through a positive angle. Further, the angle distributions seem to be symmetric (given that the small sample size leads to significant variance). Corresponding results were found for φ lying between 16° – 30° and 31° – 45° , but data were too sparse to make a study of yet larger angles meaningful.

In Fig. 2b we show the resulting $p(\theta)$ for the three angle groups $0^\circ \leq |\varphi| \leq 15^\circ$, $15^\circ \leq |\varphi| \leq 30^\circ$, $30^\circ \leq |\varphi| \leq 45^\circ$, assuming that the distributions indeed are symmetric with respect to the initial direction so that they can be superimposed for positive and negative travel. [To obtain Fig. 2b we arbitrarily choose the direction of motion prior to a turn to be (+), so that a turn towards the axis is indicated as negative (-).] Note that the distributions are of approximately the same shape, and the positions of the maxima are only weakly dependent upon φ . (Similar curves are obtained when a 10° mesh is used to form the histograms; however, the distributions vary somewhat in detail.) Conditional turn-angle distributions, as presented in Fig. 2b, are used in the theoretical analysis which follows (see Eq. 6). An alternate representation which emphasizes the slight correlation between turn *magnitude* and prior direction is shown in the scatter plot given in Fig. 2c.

For comparison, we show in Fig. 3 the histogram of a turn-angle distribution discerned for cells moving in the absence of chemoattractant, i.e. without any directional bias. Although in this case the cell sample differed from that used to determine the curves presented in Fig. 2, the results are typical of several observations. Figs. 2b and 3 suggest that the width of the turn-angle distribution seems to narrow when the cells are in a chemotactic field. On the other hand, due to the procedure used for generating chemoattractant in these studies, it was difficult to study cell motion in a spatially homogeneous environment which contained chemoattractant and it may be that the

¹ The distributions are distorted somewhat in the range $0^\circ < |\theta| < 15^\circ$ since a cell had to move more than 10° about its axis in order that an event be scored as a turn (see Zigmond, 1974).

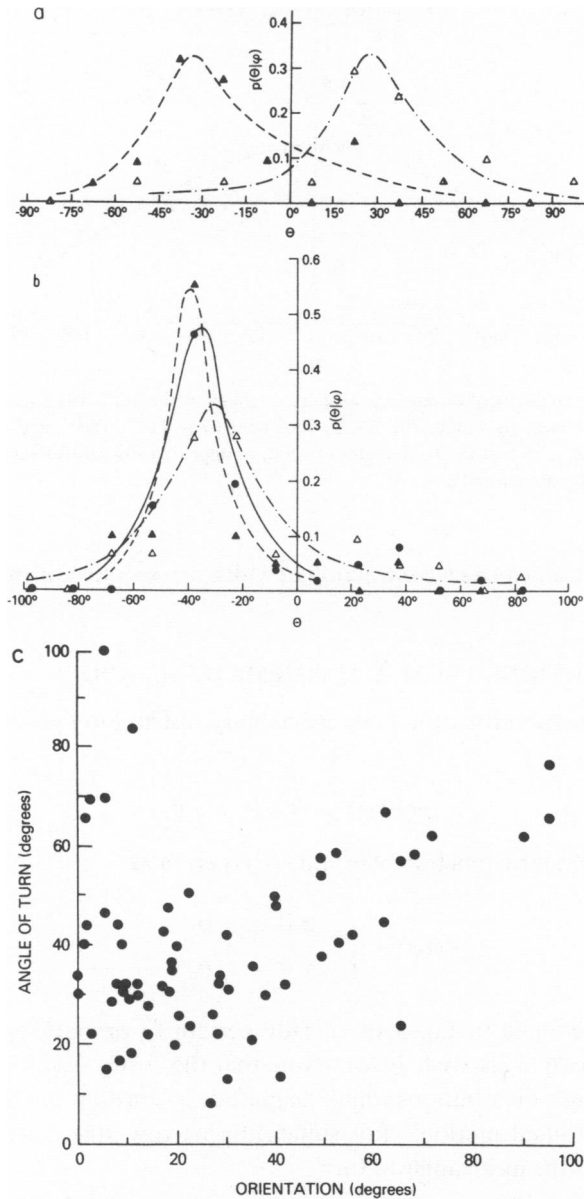


FIGURE 2 Turn-angle distributions obtained from tracking data. (a) Conditional turn-angle probability $p(\theta|\varphi)$ for turning through an angle θ when, before a turn, cells were moving at an angle lying between 0° and 15° with respect to the source axis. Cells have a strong tendency to turn in the opposite direction of their motion. (The points \blacktriangle pertain to positive angles, viz., $0^\circ < \varphi \leq 15^\circ$; the points \triangle pertaining to negative angles $-15^\circ \leq \varphi < 0^\circ$.) (b) Distribution functions $p(\theta|\varphi)$, obtained by arbitrarily taking the direction before a turn as (+), so that a turn to a (-) angle corresponds to a turn towards the source axis. These curves are superpositions of the (assumed) symmetric curves of the type shown in (a). Key: \triangle pertains to cell motion before a turn such that $0^\circ \leq |\varphi| \leq 15^\circ$; \bullet pertains to $16^\circ < |\varphi| \leq 30^\circ$; \blacktriangle pertains to $31^\circ < |\varphi| \leq 45^\circ$. (c) Scatter diagram of the magnitude of turn angles, plotted vs. the angle of locomotion before a turn.

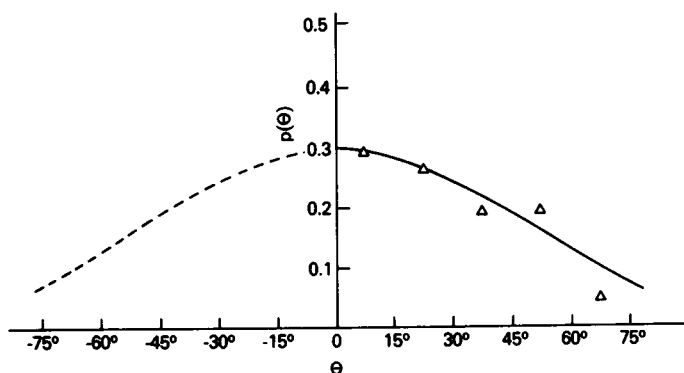


FIGURE 3 Turn-angle distribution in the absence of chemoattractant. Although the sample here differs from that used to deduce the results shown in Figs. 2*a, b*, this curve is representative of several observations that the turn-angle distribution appears to be considerably broader when cells move without directional bias.

chemoattractant itself causes a contraction in width, irrespective of the presence of the gradient.

CALCULATIONS FROM A MATHEMATICAL MODEL

To a first approximation the turn-angle probability distribution given in Fig. 2 can be represented as

$$p(\theta | \varphi) = p[\theta + f(\varphi)], \quad (6)$$

where $p(\theta)$ is a symmetric function of θ , and $f(\varphi)$ is given as

$$f(\varphi) = \begin{cases} \bar{\varphi} & \text{if } \varphi > 0. \\ -\bar{\varphi} & \text{if } \varphi < 0. \end{cases} \quad (7)$$

The equations presented in Eq. 5 specifically pertain to probability distributions of the form given in Eq. 6 (Nossal, 1976). Note that the form $f(\varphi)$ in Eq. 7 signifies a bias in the turn-angle distributions whose magnitude is constant but always oppositely directed to the original motion. For sufficiently narrow $p(\theta)$ (such as in Fig. 2*b*), $f(\varphi)$ simply equals the mean angle of turn.

The coefficients $I(m, 0, l)$ appearing in Eq. 5 have the definition (Nossal, 1976)

$$I(m, 0, l) = (2\pi)^{-1} \int_{-\pi}^{\pi} e^{-im\varphi} e^{il[\varphi - f(\varphi)]} d\varphi, \quad (8)$$

so that, for the $f(\varphi)$ given in Eq. 7, we find

$$I(m, 0, l) = \begin{cases} \{[1 - (-1)^{l-m}]/\pi(l-m)\} \sin l\bar{\varphi} & \text{if } l \neq m \\ \cos m\bar{\varphi} & \text{if } l = m \end{cases} \quad (9)$$

In general, the terms $\{\beta_i\}$ in Eq. 5 are Fourier coefficients of the angle dependence of the run-length distribution $P(\tau|\varphi)$. However, since such angle dependence seems to be insignificant for leukocyte chemotaxis, the $\{\beta_i\}$ are in this case given, trivially, as

$$\beta_i = \beta_0 \delta_{i,0}^{Kr}, \quad (10)$$

where β_0 is the first moment of the run-length distribution (Nossal, 1976). Moreover, as one might expect, β_0 does not appear in the solution for a_0 . The latter point is clarified if we recognize that Eqs. 7-10 imply that Eq. 5 can be rewritten as

$$a_0 = \frac{4}{\pi\beta_0} \sum_{l=0}^{\infty} \frac{b_{2l+1}}{2l+1} p_{2l+1} \sin \{(2l+1)\bar{\varphi}\}, \quad (11A)$$

$$b_m(1 - p_m \cos m\bar{\varphi}) = \frac{1}{2} \beta_0 \delta_{m,1}^{Kr} - \sum_{\substack{l=1 \\ l \neq m}}^{\infty} [b_l \sin l\bar{\varphi}] \frac{2lp_l}{\pi(l^2 - m^2)} [1 - (-1)^{l-m}], \quad (11B)$$

where, we recall, the $\{b_l\}$ are unknowns. The $\{p_l\}$ are determined from the turn-angle distributions, viz. (Nossal, 1976)

$$p_l = p_{-l} = \int_{-\pi}^{\pi} e^{-il\zeta} p(\zeta) d\zeta. \quad (12)$$

(To obtain Eqs. 11 we also have used the fact that $b_l = b_{-l}$.) The Kronecker delta $\delta_{m,n}^{Kr}$ has the usual meaning, viz., $\delta_{m,n}^{Kr} = 1$ if $m = n$ and is otherwise zero.²

We shall discuss the evaluation of the $\{p_l\}$ shortly. First, however, we find it convenient to define B_m , T_m , and $K_{m,l}$ as

$$B_m = 2\beta_0^{-1} \{mp_m \sin m\bar{\varphi}\} b_m, \quad (13A)$$

$$T_m = (1 - p_m \cos m\bar{\varphi}) / (mp_m \sin m\bar{\varphi}), \quad (13B)$$

$$K_{m,l} = \begin{cases} 4/\pi(l^2 - m^2) & \text{if } l + m \text{ is odd} \\ 0 & \text{if } l + m \text{ is even.} \end{cases} \quad (13C)$$

²Eq. 5 has been obtained under the assumption that velocities are not affected by the direction of movement. A simple modification is

$$\frac{1}{2} \sum_{n=-\infty}^{\infty} \{\beta_{n+1} + \beta_{n-1}\} v_{m-n} - a_0 \beta_m = \sum_{l=-\infty}^{\infty} b_l \{\delta_{l,m}^{Kr} - p_{-l} l(m, 0, l)\},$$

when the velocity distribution $p(v|\varphi)$ is angle dependent. If the Fourier representation of the latter is $p(v|\varphi) = \sum_l p_l(v) e^{il\varphi}$, the coefficient v_l is defined as $v_l = v_0 \int_0^{2\pi} v p_l(v) dv$, with $v_0 \equiv \int_0^{2\pi} v p_0(v) dv$. Note that if the velocity distribution is not dependent upon φ , $v_l = \delta_{l,0}^{Kr}$. A cursory analysis of the tracking data used to deduce Figs. 2 and 3 suggests no significant angle dependence in the velocity distribution, but a careful study has not been performed.

Some simple manipulation of Eqs. 11 then allow us to express a_0 as

$$a_0 = \frac{2}{\pi} \sum_{l=0}^{\infty} (\mathbf{A}^{-1})_{(2l+1),1} / (2l+1)^2 \quad (14)$$

where $(\mathbf{A}^{-1})_{l,m}$ is the l,m th element of the inverse of a tensor \mathbf{A} , the latter being defined in terms of the expressions given in Eq. 13 as

$$\mathbf{A} = \begin{pmatrix} T_1 & K_{12} & 0 & K_{14} & 0 & K_{16} & \dots \\ K_{21} & T_2 & K_{23} & 0 & K_{25} & 0 & \dots \\ 0 & K_{32} & T_3 & K_{34} & 0 & K_{36} & \dots \\ K_{41} & 0 & K_{43} & T_4 & K_{45} & 0 & \dots \\ \dots & \dots & \dots & \dots & \dots & \dots & \dots \end{pmatrix} \quad (15)$$

Note that the coefficient β_0 does not appear, i.e., the run length distribution does not influence $\langle \text{CI} \rangle$, even indirectly.

An approximate solution based on Eq. 14 is obtained by setting the order of \mathbf{A} to a finite value. We show in the Appendix that the expression for a_0 converges rapidly when tensors of successively higher even orders are chosen. Analytic expressions are easily derived when approximate tensors of low orders are used, and numerical results using higher order approximations are easily obtained.

At this point the coefficients $\{p_l\}$ need to be specified. A simple analytical approximation of the distribution function displayed in Fig. 2 is

$$p(\theta) = \begin{cases} \frac{1}{\theta^*} \left(1 - \frac{|\theta|}{\theta^*}\right), & |\theta| \leq \theta^* \\ 0, & |\theta| > \theta^* \end{cases} \quad (16)$$

in which case the $\{p_l\}$ are given as

$$p_l = 2[1 - \cos l\theta^*] / l^2[\theta^*]^2. \quad (17)$$

The following section contains results of calculations based on Eqs. 6, 14, and 17. Further discussion appears in the Appendix.

NUMERICAL RESULTS FOR CHEMOTROPISM INDICES

One attribute of a theoretical model is that its parameters can be manipulated to elucidate behavior which might not be readily amenable to experimental investigation. Consequently, we have computed the chemotropism index in order to gain insight into its dependence on such variables as the width of the turn-angle distribution (characterized by θ^*) and the magnitude of the bias offset angle $\bar{\varphi}$ (see Eq. 7).

In Fig. 4 we show how $\langle \text{CI} \rangle$ varies as a function of $\bar{\varphi}$ when $f(\varphi)$ and $p(\theta)$ are given by Eqs. 7 and 16, respectively. The chemotropism index increases linearly

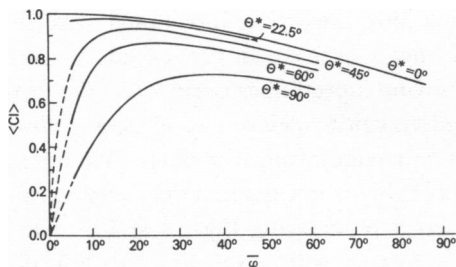


FIGURE 4

FIGURE 4 Variation of the chemotropism index $\langle CI \rangle$ when $f(\varphi)$ and $p(\theta)$ are represented by Eqs. 7 and 16. Numerical results derived from Eqs. 14 are shown as a function of bias offset angle $\bar{\varphi}$, for various turn-angle distributions of differing widths θ^* .

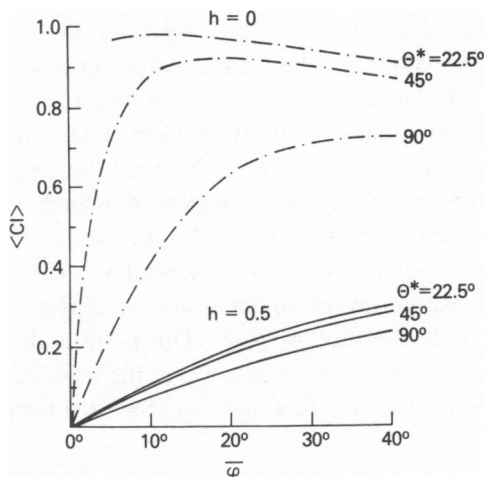


FIGURE 5

FIGURE 5 Chemotropism index when the turn-angle distribution is given as $p'(\theta) = h + (1 - h)p(\theta)$, where $h/(2\pi)$ is the height of a uniformly wide "background" component, and $p(\theta)$ is given by Eq. 16.

with $\bar{\varphi}$ for low values of mean angle of turn, maximal chemotactic response being achieved at a value whose magnitude depends on the width of $p(\theta)$. If the offset bias increases beyond this value the chemotropism index slowly decreases, reflecting the fact that for large values of $\bar{\varphi}$ the cells overcompensate on turning and tend to "zig-zag" with excessive amplitude. The transition from randomly directed motion to strong chemotactic response occurs most rapidly when the width of the turn-angle distribution is narrow (compare, for example, the curve for $\theta^* = 45^\circ$ with that for $\theta^* = 90^\circ$). Also, the achievable response depends upon the width of the turn-angle distribution—as the width increases the maximal response decreases. The latter point is corroborated in Fig. 5. There, results are shown for a situation where $p(\theta)$ contains a uniform background term in addition to the distribution given in Eq. 16 (see figure legend).

From Fig. 2 we discern $\bar{\varphi}$ to be approximately 35° and θ^* to lie between 30° and 45° . Thus, from Fig. 4 we would predict that the chemotropism index is close to 0.9. (Actually, the apparent broad "wings" of $p(\theta | \varphi)$ [see Fig. 2] imply that $\langle CI \rangle$ is somewhat lower—cf. Figs. 4, 5.) This theoretically inferred value of the chemotropism index is consistent with the experimentally determined value of 0.85 which was calculated directly from cinemicrograph projections (Zigmond, 1974).

Parenthetically, we note from Figs. 4 and 5 that, beyond a certain point, large increases in offset bias result in only small changes in the chemotropism index. Thus, if a "saturation" in chemotactic velocity were to be observed when leukocytes were

tested by macroscopic observation (e.g., in increasingly steep gradients of chemoattractant), it merely might reflect the stochastic nature of the locomotion.

The results shown in Figs. 4 and 5 imply that an efficient mechanism for effecting chemotactic response would be one which not only imparts a directional bias to $p(\theta | \varphi)$, but which also sharpens the range of angles over which turns could occur. (Preliminary evidence suggests that such a narrowing indeed does occur—see Fig. 3.) Careful experimental studies now should be undertaken to determine, in detail, how turn-angle bias functions depend on chemoattractant concentration profiles. We note, however, that observed macroscopic response probably is not qualitatively very sensitive to the form of $f(\varphi)$. This point is illustrated by comparing Figs. 4 and 6. The latter pertains to a case where the peak of $p(\theta | \varphi)$ varies with φ (cf. Fig. 2). Specifically, we have chosen $f(\varphi)$ to have the form

$$f(\varphi) = \begin{cases} \bar{\varphi} + \epsilon\varphi, & \varphi > 0 \\ -\bar{\varphi} + \epsilon\varphi, & \varphi < 0, \end{cases} \quad (18)$$

from which the results shown in Fig. 6 follow. These computations also show that vectorial turning is the predominant factor in effecting chemotactic response. Accommodation—i.e. alterations in the magnitude of the angle of turn as a function of prior orientation—makes a relatively insignificant contribution to the chemotropism index.

Lastly, we recognize that a more profound explanation of directed cell locomotion awaits elucidation of the molecular machinery which translates external chemical stimuli into requisite cytoskeletal alterations. However, the current study draws attention to the type of information about the stochastic character of cell locomotion which is needed in order to elaborate an appropriate mechanistic model. Also, we have tried to develop deeper understanding of the relationships between movement of individual leukocytes and parameters derived from measurements which are made on a collection of cells. The resulting theory allows us to examine the manner in which

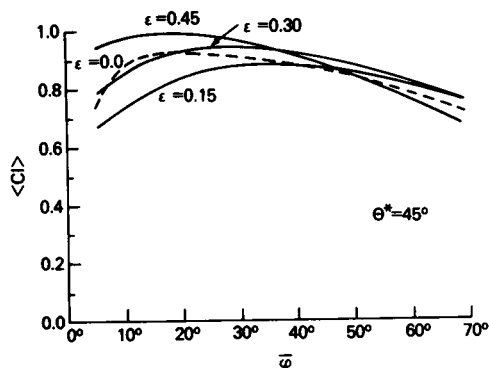


FIGURE 6 Dependence of the chemotropism index upon the offset bias angle, when the latter increases as a function of $|\varphi|$ according to Eq. 18. The turn-angle distribution $p(\theta)$ has the form given in Eq. 16, the width having the specific value $\theta^* = 45^\circ$. The values $\epsilon = 0.3$, $\bar{\varphi} = 27^\circ$, roughly correspond to the data shown in Fig. 2.

variation in cell behavior (for example, a change in magnitude of the turn-angle bias) influences net chemotactic response.

S. Zigmond is a Fellow of the Leukemia Society of America, Inc., and was partially supported by an American Cancer Society institutional grant to the Yale University Medical School.

Received for publication 18 March 1976.

APPENDIX

<CI> for Infinitely Sharp Turn-Angle Distributions

As θ^* (see Eq. 16) approaches zero, the chemotropism index tends to the values given in the uppermost curve of Fig. 4, i.e.

$$\lim_{\theta^* \rightarrow 0} \langle CI \rangle = \sin \bar{\varphi} / \bar{\varphi}. \tag{19}$$

Eq. 19 is obtained by noting that when the turn-angle distribution is infinitely sharp (i.e., $p(\theta | \varphi) \rightarrow \delta[\theta - f(\varphi)]$, where $\delta[...]$ here is the Dirac delta function), then, for a given initial angle φ_0 , the chemotropism index is

$$CI = \frac{1}{2}(\cos \varphi_0 + \cos(\varphi_0 - \varphi)) \tag{20}$$

when $f(\varphi)$ is given as in Eq. 7, above, and if the absolute value $|\varphi_0|$ is less than the magnitude of the turn-angle bias $\bar{\varphi}$. Eq. 20 reflects the fact that in this case a cell would always alternate directions, moving by strictly defined turns.

On the other hand, when the angle of initial travel exceeds $\bar{\varphi}$ the first few turns will be towards the axis until the resultant φ becomes less than $\bar{\varphi}$ in magnitude, after which the zig-

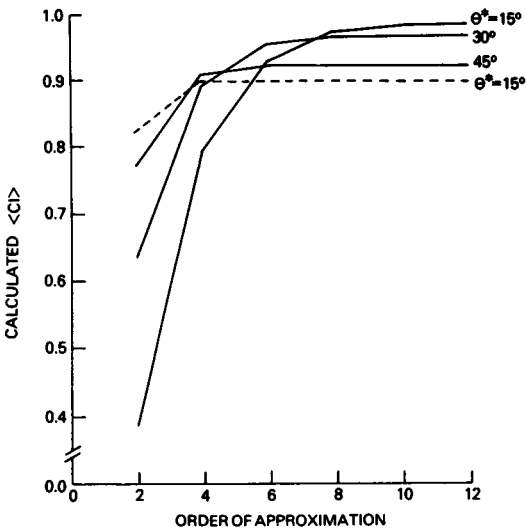


FIGURE 7 Convergence of an approximate solution of Eq. 14 obtained when $\{b_l\}$ are set equal to zero for $l > n$, n being the order of the approximation. Solid lines correspond to $\bar{\varphi} = 15^\circ$ (the number in parentheses is the exact value for $\theta^* = 0^\circ$). The dashed line pertains to $\bar{\varphi} = 30^\circ$ and exemplifies larger offset biases.

zag motion implied by Eq. 20 ensues. However, after a sufficient number of turns have elapsed such initial history contributes insignificantly to the chemotropism index. Thus, we simply can average Eq. 20 with respect to angles lying within the region defined by $\pm\bar{\varphi}$. Assuming that the distribution of φ_0 is uniform within that range, we thus find from Eq. 20 that $\langle CI \rangle$ is given as

$$\langle CI \rangle = \frac{1}{2\bar{\varphi}} \int_0^{\bar{\varphi}} [\cos \varphi_0 + \cos(\varphi_0 - \bar{\varphi})] d\varphi_0. \quad (21)$$

Eq. 19 is obtained from Eq. 21 after performing the integration.

The convergence of the approximate solution of Eq. 14 is illustrated in Fig. 7. In general, the smaller the value of θ^* , the larger the number of non-zero $\{B_i\}$ which must be used. The results shown in Figs. 4–6 were obtained by taking the order of the approximation to be $n = 12$.

REFERENCES

- BERG, H. C., and D. A. BROWN. 1972. Chemotaxis in *Escherichia coli* analyzed by three-dimensional tracking. *Nature (Lond.)* **239**:500.
- BOKISCH, V. A., H. J. MULLER-EBERHARD, and C. G. COCHRANE. 1969. Isolation of a fragment (C3a) of the third component of human complement containing anaphylatoxin and chemotactic activity and description of an anaphylatoxin inactivator of human serum. *J. Exp. Med.* **129**:1109.
- HARRIS, H. 1960. Mobilization of defensive cells in inflammatory tissue. *Bacteriol. Rev.* **24**:3.
- McCUTCHEON, M. 1923. Studies on the locomotion of leukocytes. *Am. J. Physiol.* **66**:180.
- MILLER, M. E. 1973. Cell movement and host defenses. *Ann. Intern. Med.* **78**:601.
- NOSSAL, R. 1976. Directed cell locomotion arising from strongly biased turn angles. *Math. Biosci.* **31**:121.
- NOSSAL, R., and G. H. WEISS. 1974a. A descriptive theory of cell migration on surfaces. *J. Theor. Biol.* **47**:103.
- NOSSAL, R., and G. H. WEISS. 1974b. A generalized Pearson random walk allowing for bias. *J. Stat. Phys.* **10**:245.
- PHELPS, P. 1969. Polymorphonuclear leukocyte motility *in vitro*. III. Possible release of chemotactic substance after phagocytosis of urate crystals by polymorphonuclear leukocytes. *Arthritis Rheum.* **12**:197.
- SCHIFFMANN, E., B. A. CORCORAN, and S. M. WAHL. 1975. N-formylmethionyl peptides are chemotactic for leukocytes. *Proc. Natl. Acad. Sci. U.S.A.* **72**:1059.
- SHIN, H. S., R. SNYDERMAN, E. FRIEDMAN, A. MELLERS, and M. M. MAYER. 1968. Chemotactic and anaphylatoxic fragment cleaved from the fifth component of guinea pig complement. *Science (Wash. D.C.)* **162**:361.
- STECHE, V., E. SORKIN, and G. B. RYAN. 1971. Relation between blood coagulation and chemotaxis of leukocytes. *Nature New Biol.* **233**:95.
- WARD, P. A., C. G. COCHRANE, and H. J. MULLER-EBERHARD. 1966. Further studies on the chemotactic factor of complement and its formation *in vivo*. *Immunology*. **11**:141.
- WARD, P. A., I. H. LEPOW, and L. J. NEWMAN. 1968. Bacterial factors chemotactic for polymorphonuclear leukocytes. *Am. J. Pathol.* **52**:725.
- WARD, P. A., H. G. REMOLD, and J. R. DAVID. 1969. Leukotactic factor produced by sensitized lymphocytes. *Science (Wash. D.C.)* **163**:1079.
- WILKINSON, P. C. 1974. *Chemotaxis and Inflammation*. Churchill Livingstone, Edinburgh.
- ZIGMOND, S. H. 1974. Mechanisms of sensing chemical gradients by polymorphonuclear leukocytes. *Nature (Lond.)* **249**:450.
- ZIGMOND, S. H., and J. G. HIRSCH. 1973. Leukocyte locomotion and chemotaxis. *J. Exp. Med.* **137**:387.